NUCL SCI TECH (2017) 28:85
DOI 10.1007/s41365-017-0240-9

Research on the effect of Reynolds correlation in natural convection film condensation

Lei Wu[1] · Hai-Jun Jia[1] · Xi-Zhen Ma[1] · Yang Liu[1] · Xing-Tuan Yang[1] · Jun Wang[2]

Received: 9 November 2016 / Revised: 20 April 2017 / Accepted: 21 April 2017 / Published online: 6 May 2017

Abstract Film condensation is a vital phenomenon in the nuclear engineering applications, such as the gas–steam pressurizer design, and heat removing on containment in the case of postulated accident. Reynolds number in film condensation can be calculated from either the mass relation or the energy relation, but few researches have distinguished the difference between them at present. This paper studies the effect of Reynolds correlation in the natural convection film condensation on the outer tube. The general forms of the heat transfer coefficient correlation of film condensation are developed in different flow regimes. By simultaneously solving a set of the heat transfer coefficient correlations with Re_{mass} and Re_{energy}, the general expressions for Re_{mass} and Re_{energy} and the relation between the corresponding heat transfer coefficients are obtained. In the laminar and wave-free flow regime, Re_{mass} and Re_{energy} are equivalent, while in the laminar and wavy flow regime, Re_{mass} is much smaller than Re_{energy}, and the deviation of the corresponding average heat transfer coefficients is about 30% at the maximum. In the turbulent flow regime, the relation of Re_{mass} and Re_{energy} is greatly influenced by Prandtl number. The relative deviation of their average heat transfer coefficients is the non-linear function of Reynolds number and Prandtl number. Compared with experimental results, the heat transfer coefficient calculated from Re_{energy} is more accurate.

Keywords Film condensation · Reynolds correlation · Heat transfer coefficient · Natural convection

This work was supported by Doctoral Fund of Ministry of Education of China (No. 20130002120016), the Science Found for Creative Groups of National Natural Science Foundation of China (No. 51321002), and the project of “Research and validation of key technology and device for NHR200-II nuclear heating reactor”.

✉ Yang Liu
liu_yang@tsinghua.edu.cn

Xi-Zhen Ma
cnst_xizhen@163.com

1 Institute of Nuclear and New Energy Technology, Collaborative Innovation Center of Advanced Nuclear Energy Technology, Key Laboratory of Advanced Reactor Engineering and Safety of Ministry of Education, Tsinghua University, Beijing 100084, China

2 Engineering Physics Institute, University of Wisconsin Madison, Madison, WI 53706, USA

List of symbols

C	Variable coefficient
Cp	Constant pressure-specific heat [J/(K kg)]
G	Acceleration of gravity (m/s^2)
h	Condensation heat transfer coefficient [W/(m^2 K)]
h_{fg}	Latent heat of vaporization (J/kg)
h'_{fg}	Modified latent heat of vaporization (J/kg)
$\bar{h}$	Average heat transfer coefficient [W/(m^2 K)]
k	Thermal conductivity (W/m K)
L	Length (m)
m	Variable coefficient
n	Variable coefficient
Pr	Prandtl number
Re	Reynolds number
s	Variable coefficient
T	Temperature (K)

Greek letters

μ	Viscosity (Pa s)
Γ	Mass flow rate of condensate (kg/s)
ε	Coefficient
ρ	Density (kg/m^3)

δ Thickness of condensation film (m)
Δ Difference

Subscripts

1	Laminar and wavy flow regime
2	Turbulent flow regime
b	Bulk
energy	Based on energy relation
f	Liquid phase
g	Gas phase
l	Liquid phase
mass	Based on mass relation
sat	Saturation
w	Wall

1 Introduction

Film condensation is a classical and complicated physical phenomenon, which widely exists in nuclear engineering, chemical engineering, aerospace engineering and many other fields. Many researchers have made efforts to get the accurate heat transfer coefficient correlations. The complexity in film condensation involves the following aspects: the non-equilibrium characteristics, the different modes of condensation, vapor and liquid in different flow regimes, various wall geometries and different kinds of vapors and liquids [1].

Originally, Nusselt developed a heat transfer coefficient correlation for laminar film condensation [2]. Then, Nusselt's theory was extensively improved and extended by considering the film subcooling, the inertia and drag, and the shear stress [3–6]. As an important factor in the film condensation, suction effect was found to influence the heat transfer coefficient, as high as 20% at the maximum [7]. Recently, the film condensation heat transfer in the presence of different species of non-condensable gas has been extensively studied, where the boundary layer method and the diffusion layer model were adopted [8–11]. Furthermore, Wu et al. [12] improved the diffusion layer model based on real gas-state equation, and expanded its application to the gas–steam pressurizer. In terms of the analytical model, Sin [13] developed the analytical model of film condensation in Passive Containment Cooling System(PCCS), and Mosayebidorcheh et al. [14]. used the new hybrid method to seek the analytical solution of the steady-state condensation film on the inclined rotating disk.

Many researchers verified Nusselt's theory of film condensation with the experimental results. However, large deviation occurred in the laminar and wavy flow regime and the turbulent flow regime. For this reason, many modified heat transfer coefficient correlations in film condensation were proposed [15–18]. Some semi-theoretical correlations for film condensation based on the experimental method were developed [19, 20]. One of the classic cases was developed by Butterworth [21, 22]. In the Butterworth's correlation, the whole flow regime is divided into three according to the value of Reynolds number: the laminar and wave-free flow regime, the laminar and wavy flow regime, and the turbulent flow regime. The corresponding correlations of the heat transfer coefficient in different flow regimes are given based on massive experimental databases. Many experiments have also been conducted to investigate the film condensation on the horizontal and vertical plane, inside and outside the tube, in different flow regimes, on declined condensation plane with different inclination angles, in the presence of non-condensable gas, and in different applications [23–27].

Most heat transfer coefficient correlations for the film condensation given by previous researchers are the functions of Reynolds number, or adding the modified term itself as a function of Reynolds number. Thus, the accurate calculation of Reynolds number is considered vital to obtain an accurate heat transfer coefficient. According to the basic governing equations of the film condensation, the expressions of the mass flow rate of the condensate based on the mass relation and the energy relation can be obtained, respectively. They provided two approaches to calculate the heat transfer coefficient of the film condensation. However, few researches have distinguished the differences between them, and improper applications are usually found in public researches.

In this paper, the effect of Reynolds correlation in the natural convection film condensation on outer tube is studied. Based on the general assumption of the modified term of film condensation heat transfer coefficient, the general forms of heat transfer coefficient are derived in different flow regimes. We also discover the difference between the two approaches to calculate the heat transfer coefficient of the film condensation corresponding to the different Reynolds correlations by using the analytical method and the iterative solution method. The general expressions for Re_{mass} and Re_{energy} and the relation between the corresponding heat transfer coefficients are obtained. Re_{mass} and Re_{energy} are graphically shown to see the difference. They are also used to correlate the experimental data from the open literature. It is found that the approach based on Re_{energy} is more accurate.

2 Film condensation theory

2.1 Fundamentals of condensation heat transfer

Generally, for the film condensation outside the tube, Reynolds number of the liquid film outside tube in the experiment is originally defined as

$$Re = \frac{4\Gamma}{\mu_l}. \tag{1}$$

The mass rate of condensation Γ is measurable in the experiment while calculated in the following theoretical analysis. Based on the Nusselt's theory, the expression of the condensate mass flow rate can be [28]

$$\Gamma = \frac{\rho_l(\rho_l - \rho_g)g\delta^3}{3\mu_l}. \tag{2}$$

Substituting Eq. (2) into Eq. (1), and it gives

$$Re_{\text{mass}} = \frac{4\rho_l(\rho_l - \rho_g)g\delta^3}{3\mu_l^2}. \tag{3}$$

The mass flow rate of the film condensate has another expression based on the energy relation [29], namely

$$\Gamma = \frac{\bar{h}_{\text{film}}(T_{\text{sat}} - T_w)L}{h'_{fg}}. \tag{4}$$

By substituting Eq. (4) into Eq. (1), we obtain Reynolds correlation based on energy relation as

$$Re_{\text{energy}} = \frac{4\bar{h}_{\text{film}}(T_{\text{sat}} - T_w)L}{\mu_f h'_{fg}}. \tag{5}$$

According to Nusselt's model, the correlations of heat transfer coefficient in the laminar and wavy flow regime and the turbulent flow regime are developed by adding the modified term. In this paper, we take full account of the difference of variable coefficients in the modified term and the uncertainty of the demarcation points of the different flow regimes, and obtain the general expressions of the heat transfer coefficient in three flow regimes film condensation model. The condensation film is divided into three regimes: the laminar and wave-free flow regime ($0 < Re \le Re_1$), the laminar and wavy flow regime ($Re_1 < Re \le Re_2$), and the turbulent flow regime ($Re > Re_2$), as shown in Fig. 1. The demarcation points of the film flow regimes (Re_1, Re_2) are variable.

In the laminar and wavy flow regime, the modified term (T_m) is a function of Reynolds number (Re). In the turbulent flow regime, T_m is a function of Reynolds number and Prandtl number (Re, Pr). The coefficients in the modified terms are semi-empirical parameters and usually can be treated as variable.

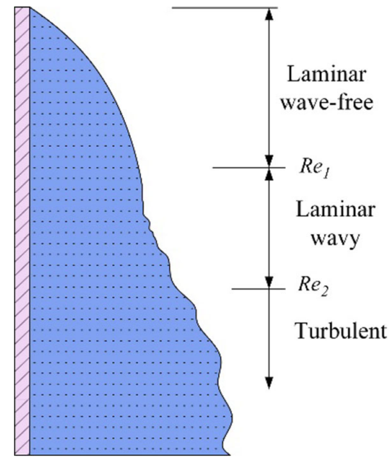

Fig. 1 Flow regimes (color online)

In the laminar and wavy-free flow regime ($0 < Re \le Re_1$), Nusselt's equation is

$$h_{\text{film}} = \left[\frac{\rho_l(\rho_l - \rho_g)g h'_{fg} k_l^3}{4\mu_l L(T_{\text{sat}} - T_w)}\right]^{1/4}. \tag{6}$$

In terms of the original Reynolds number, it can also be expressed as

$$\frac{h_{\text{film}}}{k_l}\left[\frac{\mu_l^2}{\rho_l(\rho_l - \rho_g)g}\right]^{1/3} = 1.10Re^{-1/3}. \tag{7}$$

In the laminar and wavy flow regime ($Re_1 < Re \le Re_2$) and in the turbulent flow regime ($Re > Re_2$), the modified terms are added to the basic equation of local coefficient of heat transfer in the laminar and wavy-free flow regime. The local heat transfer coefficients in all flow regimes are

$$\frac{h_{\text{film}}}{k_l}\left[\frac{\mu_l^2}{\rho_l(\rho_l - \rho_g)g}\right]^{1/3} = 1.10Re^{-1/3} \times T_m, \tag{8}$$

where the general expressions of T_m are

$$T_m = \begin{cases} 1 & 0 < Re \le Re_1 \\ m_1 Re^{n_1} & Re_1 < Re \le Re_2 \\ m_2 Re^{n_2} Pr^s & Re > Re_2 \end{cases}. \tag{9}$$

The average film condensation heat transfer coefficient is obtained by the integral average method.

$$\frac{1}{\bar{h}_{\text{film}}} = \frac{1}{Re}\int_0^{Re} \frac{1}{h_{\text{film}}} dRe. \tag{10}$$

The average heat transfer coefficients in different flow regimes are

$$\frac{\bar{h}_{\mathrm{film}}}{k_{\mathrm{l}}}\left[\frac{\mu_{\mathrm{l}}^{2}}{\rho_{\mathrm{l}}(\rho_{\mathrm{l}}-\rho_{\mathrm{g}})\mathrm{g}}\right]^{1/3}=\begin{cases}1.47Re^{-1/3} & 0<Re\le Re_1\\ \dfrac{Re}{\left[\dfrac{1}{1.1m_1\left(\dfrac{4}{3}-n_1\right)}\left(Re^{\left(\frac{4}{3}-n_1\right)}-Re_1^{\left(\frac{4}{3}-n_1\right)}\right)+0.68Re_1^{\frac{4}{3}}\right]} & Re_1<Re\le Re_2\\ \dfrac{Re}{\left[\dfrac{1}{1.1m_2\left(\dfrac{4}{3}-n_2\right)}\overset{-s}{\mathrm{Pr}}\left(Re^{\left(\frac{4}{3}-n_2\right)}-Re_2^{\left(\frac{4}{3}-n_2\right)}\right)+Re_{\mathrm{m}}\right]} & Re>Re_2\end{cases}, \tag{11}$$

where

$$Re_{\mathrm{m}}=\frac{1}{1.1m_1\left(\frac{4}{3}-n_1\right)}\left(Re_2^{\left(\frac{4}{3}-n_1\right)}-Re_1^{\left(\frac{4}{3}-n_1\right)}\right)+0.68Re_1^{\frac{4}{3}}. \tag{12}$$

The subcooling of the condensate and temperature jump across the film [28] should be taken into account when the latent heat, h'_{fg}, is calculated, as given by

$$h'_{\mathrm{fg}}=h_{\mathrm{fg}}\left[1+0.68\frac{C_{\mathrm{pl}}(T_{\mathrm{sat}}-T_{\mathrm{w}})}{h_{\mathrm{fg}}}\right]. \tag{13}$$

The temperature jump across the condensate is considered when calculating the temperature of liquid film [28].

$$T_{\mathrm{film}}=T_{\mathrm{w}}+0.25(T_{\mathrm{sat}}-T_{\mathrm{w}}). \tag{14}$$

As seen from Eqs. (3) and (5), Re_{energy} contains the average heat transfer coefficient $\bar{h}_{\mathrm{film}}$, whereas Re_{mass} is a function of the thickness of the film condensate, which corresponds to the local heat transfer coefficient h_{film}. In consideration of Eqs. (7) and (11), it is indicated that it provides two approaches to calculate the heat transfer coefficient of the film condensation and Reynolds number, such as pair parameters of ($\bar{h}_{\mathrm{film}}$, Re_{energy}) and (h_{film}, Re_{mass}). However, the fundamental difference between these two approaches still remains unclear when applied to calculate the film condensation heat transfer coefficient.

2.2 Theoretical analysis of Re_{mass} and Re_{energy}

Under the same thermal hydraulic parameter condition, these two approaches of calculating the film condensation heat transfer coefficient are used to obtain the general expressions for Re_{mass} and Re_{energy} in different flow regimes.

In the laminar and wave-free flow regime, combining Eqs. (3), (5), (6) and (11), Re_{mass} and Re_{energy} are equivalent and given as

$$Re_{\mathrm{mass}}=Re_{\mathrm{energy}}=3.776\left[\frac{\rho_{\mathrm{l}}(\rho_{\mathrm{l}}-\rho_{\mathrm{g}})\mathrm{g}\mathrm{k}_{\mathrm{l}}^{3}\mathrm{L}^{3}(\mathrm{T}_{\mathrm{sat}}-\mathrm{T}_{\mathrm{w}})^{3}}{\mu_{\mathrm{l}}^{5}h_{\mathrm{fg}}'^{3}}\right]^{1/4}. \tag{15}$$

In laminar and wavy flow regime, the similar approach in the laminar and wavy-free flow regime is also presented. Equations (3), 7 and (9) may be combined to provide

$$Re_{\mathrm{mass}}=C_{11}\left(\frac{\rho_{\mathrm{l}}(\rho_{\mathrm{l}}-\rho_{\mathrm{g}})\mathrm{g}k_{\mathrm{l}}^{3}L^{3}(T_{\mathrm{sat}}-T_{\mathrm{w}})^{3}}{\mu_{\mathrm{l}}^{5}h_{\mathrm{fg}}'^{3}}\right)^{\frac{1}{4(3n_1+1)}}. \tag{16}$$

Inserting Eqs. (5) and (11), it provides an expression for Re_{energy}.

$$Re_{\mathrm{energy}}=\left[\frac{4}{C_{13}}\left(\frac{\rho_{\mathrm{l}}(\rho_{\mathrm{l}}-\rho_{\mathrm{g}})\mathrm{g}L^{3}k_{\mathrm{l}}^{3}(T_{\mathrm{sat}}-T_{\mathrm{w}})^{3}}{\mu_{\mathrm{l}}^{5}h_{\mathrm{fg}}'^{3}}\right)^{1/3}+\frac{C_{12}}{C_{13}}\right]^{\frac{1}{\frac{4}{3}-n_1}}, \tag{17}$$

where

$$C_{11}=\left(\frac{4}{3m_1^3}\right)^{\frac{1}{3n_1+1}}4^{\frac{3}{4(3n_1+1)}},\ C_{12}=\frac{1}{1.1m_1\left(\frac{4}{3}-n_1\right)},\ C_{13}=0.68Re_1^{\frac{4}{3}}-\frac{Re_1^{\left(\frac{4}{3}-n_1\right)}}{1.1m_1\left(\frac{4}{3}-n_1\right)}.$$

Substituting Eq. (17) into Eq. (16), the relation between Re_{mass} and Re_{energy} in the laminar and wavy flow regime would be given as

$$Re_{\mathrm{mass}}=C_{11}\left(\frac{C_{12}}{4}Re_{\mathrm{energy}}^{\left(\frac{4}{3}-n_1\right)}-\frac{C_{13}}{4}\right)^{\frac{3}{4(3n_1+1)}}. \tag{18}$$

In the turbulent flow regime, Re_{mass} and Re_{energy} are given as

$$Re_{\mathrm{mass}} = C_{21}\left[Pr^{-3s}\left(\frac{\rho_l(\rho_l-\rho_g)gk_l^3L^3(T_{\mathrm{sat}}-T_w)^3}{\mu_l^5h_{fg}'^3}\right)^{\frac{1}{4}}\right]^{\frac{1}{3n_2+1}}, \tag{19}$$

$$Re_{\mathrm{energy}} = \left[\frac{4Pr^s}{C_{21}}\left(\frac{\rho_l(\rho_l-\rho_g)gL^3k_l^3(T_{\mathrm{sat}}-T_w)^3}{\mu_l^5h_{fg}'^3}\right)^{1/3} - \frac{C_{23}}{C_{22}}Pr^s + Re_2^{\left(\frac{4}{3}-n_2\right)}\right]^{\frac{1}{\left(\frac{4}{3}-n_2\right)}}, \tag{20}$$

where

$$C_{21} = \left(\frac{4}{3m_2^3}\right)^{\frac{1}{3n_2+1}}4^{\frac{3}{4(3n_2+1)}},\ C_{22} = \frac{1}{1.1m_2\left(\frac{4}{3}-n_2\right)},\ C_{23} = \frac{1}{1.1m_1\left(\frac{4}{3}-n_1\right)}\left(Re_2^{\frac{4}{3}-n_1} - Re_1^{\frac{4}{3}-n_1}\right) + 0.68Re_1^{\frac{4}{3}},$$

By substituting Eq. (20) into Eq. (19), we can get the relation between Re_{mass} and Re_{energy} in the turbulent flow regime.

$$Re_{\mathrm{mass}} = C_{21}\left[\frac{C_{22}}{4}Pr^{-5s}\left(Re_{\mathrm{energy}}^{\left(\frac{4}{3}-n_2\right)} - Re_2^{\left(\frac{4}{3}-n_2\right)}\right) + \frac{C_{23}}{4}Pr^{-4s}\right]^{\frac{3}{4(3n_2+1)}}. \tag{21}$$

2.3 Relation of Re_{mass} and Re_{energy} in Butterworth's case

For further analysis, the coefficients of the Butterworth's correlation are adopted as an example for Eqs. (18) and (21) (Table 1).

By substituting all these parameters into Eqs. (18) and (21), the relations between Re_{mass} and Re_{energy} in different flow regimes can be obtained.

In the laminar and wave-free flow regime

$$Re_{\mathrm{mass}} = Re_{\mathrm{energy}}. \tag{22}$$

In the laminar and wavy flow regime

$$Re_{\mathrm{mass}} = \left(7.12Re_{\mathrm{energy}}^{1.22} - 34.29\right)^{0.564}. \tag{23}$$

Table 1 Variable coefficients in Butterworth's correlation

Parameter	m_1	n_1	m_2	n_2	s	Re_1	Re_2
Value	0.6868	0.11	0.2091	7/12	1/2	30	1600

In the turbulent flow regime

$$Re_{\mathrm{mass}} = 228.40\left(Re_{\mathrm{energy}}^{0.75}Pr^{-2.5} + 150.86Pr^{-2.0} - 253Pr^{-2.5}\right)^{0.2727}. \tag{24}$$

Under the same thermal hydraulic parameter condition, the relation of Re_{mass} and Re_{energy} is significantly different in each flow regime. Obviously, Re_{mass} and Re_{energy} are equivalent in the laminar and wavy-free regime. However, Fig. 2 shows the relation between Re_{mass} and Re_{energy} in the laminar and wavy flow regime and the turbulent flow regime, described by Eqs. (23) and (24).

From Fig. 2a, we can see there is a significant difference between Re_{mass} and Re_{energy} in the laminar and wavy regime. Under the same thermal hydraulic parameter condition, Re_{energy} keeps higher than Re_{mass} (maximally 4 times). Prandtl number does not play a role in this flow regime.

In the turbulent flow regime, Prandtl number significantly influences the relation between Re_{mass} and Re_{energy} (see the line of Re_{mass}–Re_{energy} in Fig. 2b). Considering the crosspoint of $Re_{\mathrm{mass}} = Re_{\mathrm{energy}}$ and Re_{mass}–Re_{energy}, there is an obvious demarcation point at Prandtl number, 0.35. When Prandtl number is less than 0.35, the lines of $Re_{\mathrm{mass}} = Re_{\mathrm{energy}}$ and Re_{mass}–Re_{energy} intersect at one point, and $Re_{\mathrm{mass}} < Re_{\mathrm{energy}}$ and $Re_{\mathrm{mass}} > Re_{\mathrm{energy}}$ are presented on either side of the crosspoint. When Prandtl number is larger than 0.35, the line of Re_{mass}–Re_{energy} deviates heavenly from that of $Re_{\mathrm{mass}} = Re_{\mathrm{energy}}$ as Prandtl number increasing, and $Re_{\mathrm{mass}} < Re_{\mathrm{energy}}$. In particular, when Prandtl number increases to about 0.8 or more, $30 < Re_{\mathrm{mass}} < 1600$, corresponding to the laminar and wavy regime; whereas, $Re_{\mathrm{energy}} > 1600$, the corresponding flow regime is the turbulent flow regime. In conclusion, Prandtl number greatly influences the relation between Re_{mass} and Re_{energy}, and their large deviation occurs in the turbulent flow regime.

We can also obtain the heat transfer coefficient and Reynolds number, such as (h_{film}, Re_{mass}) and ($\bar{h}_{\mathrm{film}}$, Re_{energy}), in different flow regimes by using the iterative solution method. The iterative calculation flow chart is shown in Fig. 3.

According to the result of h_{film} and Re_{mass}, we can obtain $\bar{h}_{\mathrm{mass}}$ by using the average method of Eq. (10). Define the relative deviation of the average heat transfer coefficient as:

$$\varepsilon = \frac{\bar{h}_{\mathrm{mass}} - \bar{h}_{\mathrm{energy}}}{\bar{h}_{\mathrm{energy}}} \times 100\%. \tag{25}$$

This definition of relative deviation not only presents its relative magnitude, but also directly shows whether it is positive or negative.

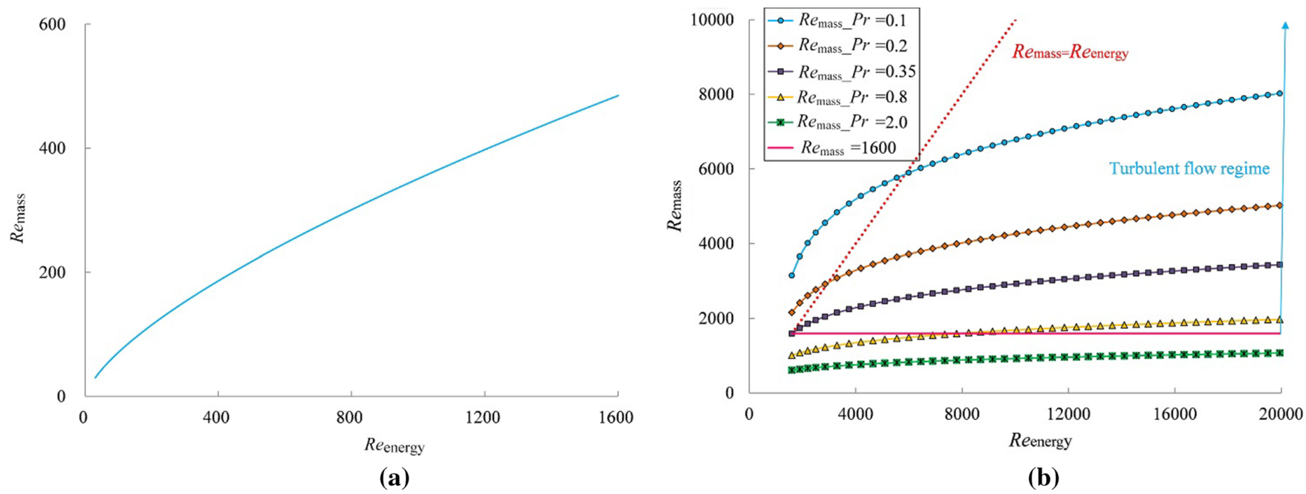

Fig. 2 (Color online) Relation between Re_{mass} and Re_{energy}

Fig. 3 Iterative calculation flow chart

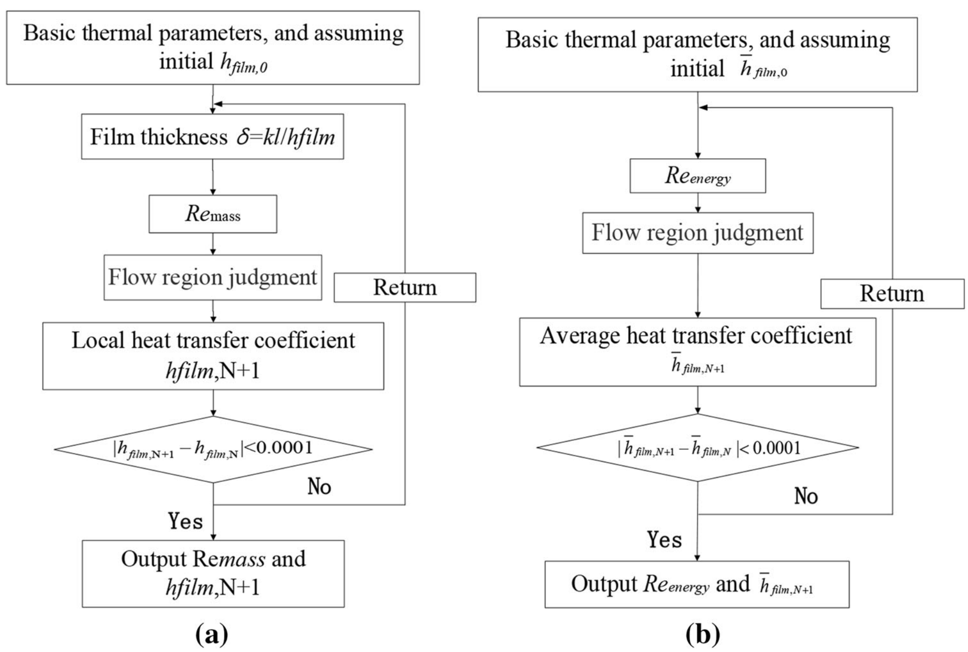

According to Eqs. (22) and (25), $\varepsilon = 0$ in the laminar and wave-free flow regime, and it means that $\bar{h}_{\text{mass}}$ and $\bar{h}_{\text{energy}}$ are equivalent.

In the laminar and wavy flow regime, the value of ε is positive, as shown in Fig. 4a. The maximum deviation is as high as 30%, corresponding to Re_{energy} of 1600. It means that $\bar{h}_{\text{mass}} > \bar{h}_{\text{energy}}$ exists in the whole laminar and wavy flow regime.

Figure 4b shows a complicated situation in the turbulent flow regime, and ε is a highly nonlinear function of Reynolds number and Prandtl number. When Prandtl number is less than 0.35, there are two intersections of the curve of ε and the horizontal coordinate. The value of ε is alternately negative, positive and negative, with the increase in Reynolds number; $\bar{h}_{\text{mass}} < \bar{h}_{\text{energy}}$ and $\bar{h}_{\text{mass}} > \bar{h}_{\text{energy}}$ alternately present in low, moderate and high Reynolds number regime. The minimum value of ε is larger than -60%, corresponding to $Pr = 0.1$ and $Re_{\text{energy}} = 1600$. When Prandtl number is larger than 0.35, ε monotonously decreases from positive value to negative value as Reynolds number increasing, and there is only one crosspoint of $\varepsilon = 0$. When Prandtl number increases from 0.35 to 4.0, the value of ε increases from 0 to 35% in the low Reynolds number region ($1600 < Re < 4000$), the maximum value of ε is less than 60%, and the Re_{energy} value corresponding to the crosspoint of $\varepsilon = 0$ decreases from 12,000 to 4000. In conclusion, when $0.1 < Pr < 4.0$, ε is generally within the range of -60 to $+60\%$, and it is a highly nonlinear

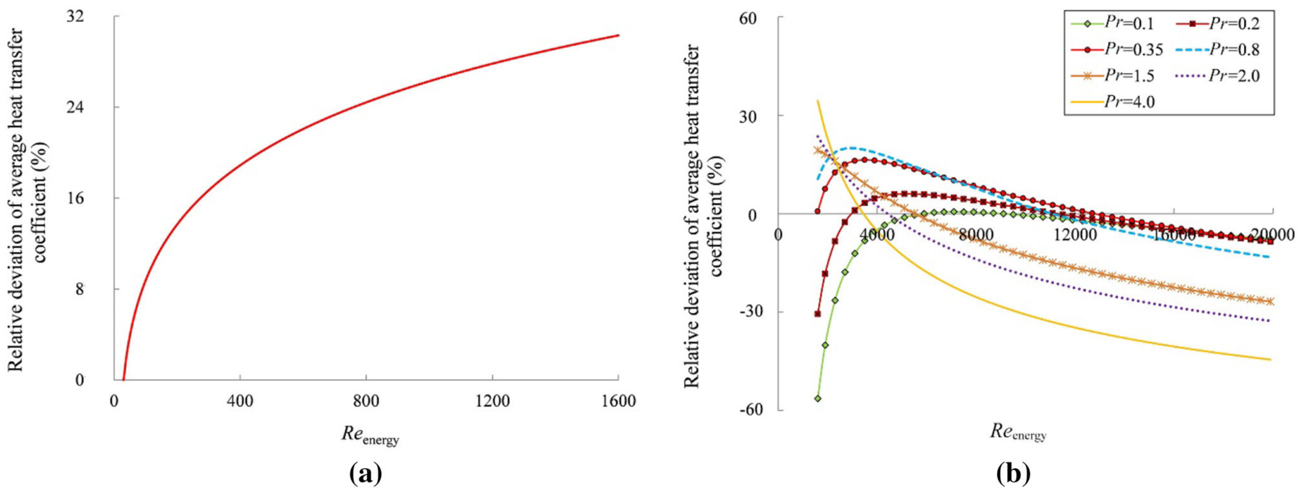

Fig. 4 (Color online) Relative deviation of average heat transfer coefficient

Table 2 Experimental parameters

Parameters in the experiment	Value
Species of gas	Vapor
Total pressure	Atmospheric pressure
Temperature difference between bulk and wall	10–35 K
Inclined angle	90°
Effective length	0.09 m
Convection in bulk	Natural

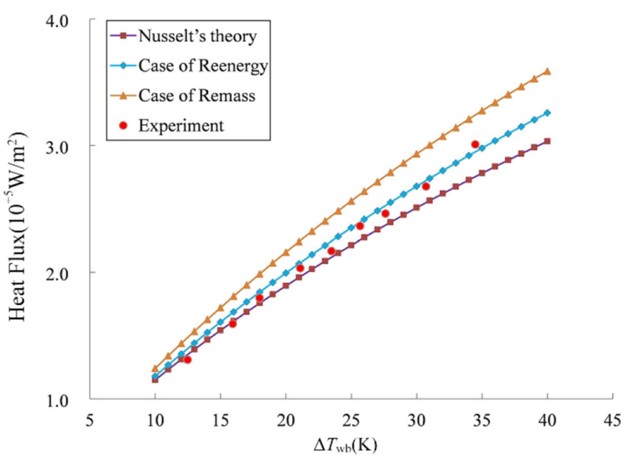

Fig. 5 (Color online) Heat flux with temperature difference between wall and bulk

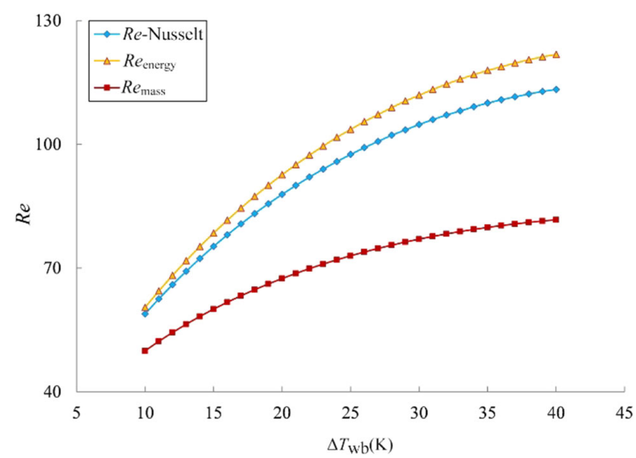

Fig. 6 (Color online) Reynolds number with temperature difference between wall and bulk

function of Reynolds number and Prandtl number in the turbulent flow regime.

3 Experiment validation

Experimental results from Chung et al. [15] and Hebbard and Badger [18] are used to verify the accuracy of the two Reynolds correlations.

The experiment set by Chung et al. [15] focuses on the film wise and drop wise condensation of steam on short inclined plates. Table 2 shows the experiment conditions.

The result is shown in Figs. 5 and 6. The heat flux and Reynolds number vary according to the temperature difference between wall and bulk. The result of the Nusselt's theory case is obtained from the basic Nusselt's theory in the laminar and wave-free flow regime [Eqs. (6) or (7)], and the modified term (T_m) is not taken into account in all flow regimes. It is just a reference case.

It shows that the heat flux calculated with Re_{energy} has a good agreement with the experimental data, especially in high temperature difference region. The result obtained with Re_{mass} over-predicted the test results at an average deviation of 11.0%. The heat flux calculated from Nusselt's theory is lower than the experimental results, and the deviation increases as ΔT_{wb} increasing. However, when ΔT_{wb} is small (10 K < ΔT_{wb} < 16 K) in this experiment, Nusselt's theory can effectively predict the heat flux, while the method using Re_{energy} slightly over-predicted the results. Major reason is that Reynolds number corresponding to this condition is less than 80 (Fig. 6), and Nusselt's theory can be effective in the wavy-weak flow regime. Re_{mass} and Re_{energy} at the same ΔT_{wb} are quite different, as shown in Fig. 5. The average deviation Reynolds number between Re_{energy} and Nusselt's theory is within 10%. It is consistent with the theoretical analysis in the part II-C.

In conclusion, the calculating approach based on Re_{energy} promises a better performance in the low Reynolds number regime.

Another pure steam condensation experiment performed by Chung et al. [15] is selected to assess the Reynolds correlation in the laminar and wavy flow regime and the turbulent flow regime. The experimental conditions are listed in Table 3.

When the bulk temperature varies from 353.15 to 393.15 K, Reynolds number is generally located in the laminar and wavy flow regime and the turbulent flow regime. According to the value of Reynolds number, different correlations are used for various flow regimes to determine the film condensation heat transfer coefficient. The result is shown in Fig. 7.

Form Fig. 7, in the case of different steam temperature, the value curve of the heat transfer coefficient with Re_{energy} is always located between the value curve of the heat transfer coefficient with Re_{mass} and that of the heat transfer coefficient with Nusselt's theory. Furthermore, the heat transfer coefficient with Re_{mass} is maximum. The experimental data are also sandwiched between the value curves of the heat transfer coefficient with Re_{mass} and Nusselt's theory, and accords well with the heat transfer coefficient with Re_{energy}. It is indicated that when the steam temperature changes, the calculations with Re_{energy} always show a great accuracy. However, the heat coefficients are over-predicted by Re_{mass} and underestimated by Nusselt's theory.

It is necessary to point out that when ΔT_{wb} is small (3 K < ΔT_{wb} < 7 K), the predictions based on Re_{mass} fit the experimental data better, whereas when ΔT_{wb} is higher (7 K < ΔT_{wb} < 25 K), namely in the turbulent flow regime, the results based on Re_{energy} are more accurate. In this experiment, the pure steam in the bulk is not solely under natural convection, but slowly driven by external force. This is the main reason why the predictions based on Re_{mass} fit the experimental data better when ΔT_{wb} is small. When ΔT_{wb} is small, the condensation film is thin, and the weak forced convection is still influential and enhances the heat transfer coefficient. When ΔT_{wb} is larger and the condensation film becomes thicker, this effect becomes insignificant as the forced convection is no longer dominant. Thus, when ΔT_{wb} is small, the experiment results are slightly higher than the heat transfer coefficient of natural convection, which is similar to the prediction of Re_{energy}. But they are closer to the lager-predicted result calculated from Re_{mass}. In the natural convection of film condensation, the prediction of Re_{energy} is more accurate.

In addition, there may be a gradual transition between Re_{mass} and Re_{energy} cases when ΔT_{wb} is small, and the experimental value locates in the transition regime. The validation of this gradual transition will be our further study in the future.

According to the previous analysis, Reynolds correlation influences not only the heat transfer coefficient, but also the calculation of the value itself, as they are defined based on different principles, namely the mass relation and the energy relation. The approach based on Re_{energy} is a better form of formula when calculating the condensation heat transfer coefficient.

Table 3 Experimental conditions

Parameters in the experiment	Value
Species of gas	Vapor
Steam temperature	333.15–393.15 K
Temperature difference between bulk and wall	5–25 K
Inclined angle	90°
Effective length of tube	3.657 m
Diameter of tube	0.0254 m

4 Conclusion

This paper mainly discusses the effect of the Reynolds correlation on the prediction of heat transfer coefficients in the natural convection film condensation in different flow regimes.

For the natural convection film condensation on the outer wall of tube, the general forms of the heat transfer coefficient correlation are developed in different flow regimes, which can be applied in a wide range of

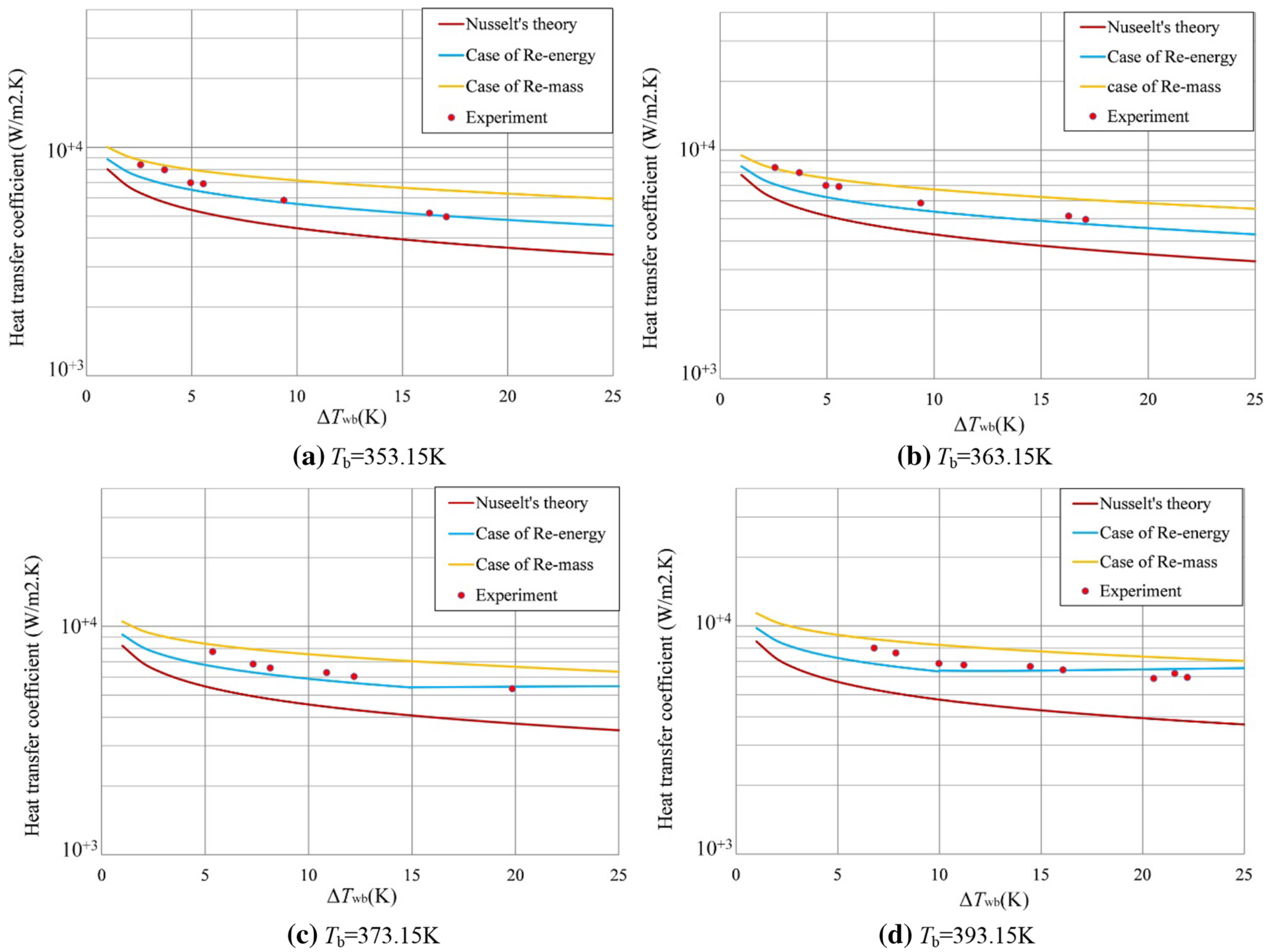

Fig. 7 (Color online) Heat transfer coefficient with different steam temperature. **a** $T_b = 353.15$ K, **b** $T_b = 363.15$ K, **c** $T_b = 373.15$ K, and **d** $T_b = 393.15$ K

conditions. The difference between the two approaches to calculating the heat transfer coefficient of the film condensation corresponding to Re_{mass} and Re_{energy} is distinguished by using the analytical method and the iterative solution method. The general expressions for Re_{mass} and Re_{energy} and the relation of the corresponding average heat transfer coefficients are also obtained for three different flow regimes. In the laminar and wave-free flow regime, Re_{mass} and Re_{energy} are equivalent. In the laminar and wavy flow regime, Re_{mass} is much smaller than Re_{energy}, and the maximal deviation of the average heat transfer coefficients from the two Reynolds correlations is as high as about 30%. In the turbulent flow regime, Prandtl number greatly influences the relation between Re_{mass} and Re_{energy}. Compared with the experimental results, the approach based on Re_{energy} turns out to be a good choice to calculate the heat transfer coefficient.

References

1. J.W. Rose, Condensation heat transfer fundamentals. Chem. Eng. Res. Des. **76**(2), 143–152 (1998). doi:10.1205/026387698524712
2. W. Nusselt, The condensation of steam on cooled surfaces. Z. Ver. Dtsch. Ing. **60**, 541–546 (1916)
3. W.M. Rohsenow, Heat transfer and temperature distribution in laminar film condensation. Trans. Asme. **78**, 1645–1648 (1956)
4. E.M. Sparrow, J.L. Gregg, A boundary layer treatment of laminar film condensation. J. Heat Transf. **81**(1), 13–18 (1959)
5. W.J. Minkowycz, E.M. Sparrow, Condensation heat transfer in the presence of noncondensables, interfacial resistance, superheating, variable properties, and diffusion. Int. J. Heat Mass Transf. **9**(10), 1125–1144 (1966). doi:10.1016/0017-9310(66)90035-4
6. E.M. Sparrow, S.H. Lin, Condensation heat transfer in the presence of a non-condensable gas. J Heat Transf. **86**(3), 430–436 (1964). doi:10.1115/1.3688714
7. L.E. Herranz, A. Campo, Adequacy of the heat-mass transfer analogy to simulate containment atmospheric cooling in the new generation of advanced nuclear reactors: experimental

confirmation. Nucl. Technol. **139**(3), 221–232 (2002). http://www.ans.org/store/article-3315/
8. J.C.Y. Koh, An integral treatment of two-phase boundary layer in film condensation. J Heat Transf. **83**(3), 359–362 (1961). doi:10.1115/1.3682285
9. V.E. Denny, A.F. Mills, V.J. Jusionis, Laminar film condensation from a steam-air mixture undergoing forced flow down a vertical surface. J Heat Transf. **93**(3), 297–304 (1971). doi:10.1115/1.3449814
10. M.H. Kim, M.L. Corradini, Modeling of condensation heat transfer in a reactor containment. Nucl. Eng. Des. **118**(2), 193–212 (1990). doi:10.1016/0029-5493(90)90057-5
11. P.F. Peterson, Theoretical basis for the Uchida correlation for condensation in reactor containments. Nucl. Eng. Des. **162**(2), 301–306 (1996). doi:10.1016/0029-5493(95)01125-0
12. L. Wu, Y. Liu, H.J. Jia, Improved diffusion layer model based on real gas state equation for high pressure condensation. Ann. Nucl. Energy **85**, 444–452 (2015). doi:10.1016/j.anucene.2015.05.006
13. S. Kima, Y.G. Lee, D.W. Jerng, Laminar film condensation of saturated vapor on an isothermal vertical cylinder. Int. J. Heat Mass Transf. **83**, 545–551 (2015). doi:10.1016/j.ijheatmasstransfer.2014.12.009
14. S. Mosayebidorcheh, T. Mosayebidorcheh, M.M. Rashidi, Analytical solution of the steady state condensation film on the inclined rotating disk by a new hybrid method. Sci. Res. Essays **9**(12), 557–565 (2014). doi:10.13140/2.1.4464.2241
15. B.J. Chung, M.C. Kim, M. Ahmadinejad, Film-wise and drop-wise condensation of steam on short inclined plates. J. Mech. Sci. Technol. **22**(1), 127–133 (2008). doi:10.1007/s12206-007-1015-8
16. L. Slegers, R.A. Seban, Laminar film condensation of steam containing small concentrations of air. Int. J. Heat Mass Transf. **13**(12), 1941–1947 (1970). doi:10.1016/0017-9310(70)90094-3
17. S.S. Kutateladze, I.I. Gogonin, Heat transfer in film condensation of slowly moving vapor. Int. J. Heat Mass Transf. **22**(12), 1593–1599 (1979). doi:10.1016/0017-9310(79)90075-9
18. G.M. Hebbard, W.L. Badger, Steam-film heat transfer coefficients for vertical tubes. Ind. Eng. Chem. **26**(4), 420–424 (1934). doi:10.1021/ie50292a013
19. J.W. Rose, Fundamentals of condensation heat transfer-Laminar film condensation. JSME Int. J. **31**, 357–375 (1988). http://ci.nii.ac.jp/naid/110002494180/
20. X.Y. Wei, X.D. Fang, R.R. Shi, A comparative study of heat transfer coefficients for film condensation. Energy Sci. Technol. **3**(1), 1–9 (2012). http://www.cscanada.net/index.php/est/article/view/2344
21. G. Neiils, S. Kliein, *Heat transfer* (Cambridge University Press, Cambridge, 2009), pp. 799–806
22. H. Uchida, A. Oyama, Y. Togo, Evaluation of post-incident cooling systems of light water power reactors. (Tokyo University, 1964). http://www.osti.gov/scitech/biblio/4023463
23. A.A. Dehbi, The effects of noncondensable gases on steam condensation under turbulent natural convection conditions. (Massachusetts Institute of Technology, 1991). http://dspace.mit.edu/handle/1721.1/13905
24. M.H. Anderson, L.E. Herranz, M.L. Corradini, Experimental analysis of heat transfer within the AP600 containment under postulated accident conditions. Nucl. Eng. Des. **185**(2), 153–172 (1998). doi:10.1016/S0029-5493(98)00232-5
25. J.W. Kim, Y.G. Lee, H.K. Ahn et al., Condensation heat transfer characteristic in the presence of noncondensable gas on natural convection at high pressure. Nucl. Eng. Des. **239**(4), 688–698 (2009). doi:10.1016/j.nucengdes.2008.12.011
26. R.I. Pashkevich, P.V. Muratov, Film condensation in a large diameter tube with upward steam flow. Int. J. Heat Mass Transf. **81**, 804–810 (2015). doi:10.1016/j.ijheatmasstransfer.2014.11.001
27. M. Kondo, H. Nakamura, Y. Kukita et al., Primary-side two-phase flow and heat transfer characteristics of a horizontal-tube PCCS condenser. In 14th International Conference on Nuclear Engineering, Miami. 2006, pp. 685–693. doi:10.1115/ICONE14-89652
28. J.G. Collier, J.R. Thome, *Convective boiling and condensation* (Oxford University Press, Oxford, 1994), pp. 445–450
29. T.L. Bergman, A.S. Lavine, F.P. Incropera et al., *Fundamentals of Heat and Mass Transfer*, 7th edn. (Wiley, Hoboken, 2011), pp. 675–679